Numerical Study of Fluid Flow and Heat Transfer over a Bank of Oval-Tubes Heat Exchanger with Vortex Generators

Abdulmajeed A. Ramadhan
Department of Mechanical Engineering- College of Engineering
University of Anbar

ABSTRACT

The present work represents a two-dimensional numerical investigation of forced laminar flow heat transfer over a 3-rows oval-tube bank in staggered arrangement with rectangular longitudinal vortex generators (LVGs) placed behind each tube. *The effects of Reynolds number (from 250 to 1500), the positions* (3 in x-axis and 2 in y-axis) *and angles of attack (*30° *and* 45°*) of rectangular VGs are examined.* The study focuses on the Influence of the different parameters of VGs on heat transfer and fluid flow characteristics of three rows oval-tube banks. The characteristics of average Nu number and skin friction coefficient are studied numerically by the aid of the computational fluid dynamics (CFD) commercial code of FLUENT 6.3. The results showed increasing in the heat transfer and skin friction coefficient with the increasing of Re number and decreasing the relative distance of positions of LVGs. It has been observed that the overall Nu_{av} number of three oval-tubes increases by *10–20.4%* and *by 10.4–27.7% with angles of* 30° and 45° *respectively, with* increasing in *the overall average of* skin friction coefficient *of three oval-tubes* reached to *53% and 72% with two angles used respectively, in comparison with the case* without VGs.

Keywords: Heat transfer enhancement, oval-tube banks, vortex generators.

1. INTRODUCTION

The compact heat exchanger is widely used in many fields such as automobile, air conditioning, power system, chemical engineering, electronic chip cooling and aerospace, etc. The main subject to design the compact heat exchanger is how to enhance the heat transfer so that its integral performance may be improved to meet the demand of high efficiency (energy saving) and low cost with the volume as small as possible and the weight as light as possible. Many studies have been carried out and many methods have been applied to the heat transfer enhancement in the compact heat exchanger since 1960s.

In compact heat exchangers, the thermal resistance of the air-side is generally dominant and may account for 80% or more of the total thermal resistance. As we know, how to reduce the thermal resistance is the key for the heat transfer enhancement. One frequently used method for heat transfer enhancement employs surfaces that are interrupted periodically along the stream wise direction. Typically, these surfaces are in the form of wavy, louver, slit, or offset strip fins. Despite the fact that interrupted surfaces can significantly improve the heat transfer performance, the associated penalty of pressure drop is also tremendous.

Another common method is to apply vortex generators (VGs), such as ribs, obstacles, wings and winglets. Vortex generators usually are incorporated into a surface by means of embossing,

stamping, punching, or attachment process. They generate longitudinal vortices, which swirl the primary flow and increase the mixing of downstream regions. In addition, the vortex generator determines the secondary flow pattern. Thus, heat transfer enhancement is associated with the secondary flow with relatively low penalty of pressure drop.

The first literature reporting the enhancement of heat transfer of using surface protrusion vortex generators is by Edwards and Alker [1]. They noted a maximum increase in the local Nusselt number of 40%. Russell et al. [2] presented the first study on the air-side heat transfer enhancement using vortex generators for the heat exchanger. The numerical studies by Biswas et al. [3] and Jahromi et al. [4] showed that the heat transfer in the wake region can be enhanced significantly in the presence of winglet type longitudinal vortex generators behind the tubes.

Extensive studies have been done on heat transfer characteristics and flow structure for heat exchangers with longitudinal vortex generators (LVGs). In recent years, the application of vortex generators in compact heat exchangers has received more and more attention.

An experimental study was conducted by Torii et al. [5] to obtain heat transfer and pressure loss in a fin-and-tube heat exchanger with in-line or staggered tube banks with delta winglet vortex generators of various configurations. The winglets were placed in a special orientation to augment heat transfer and reduce form drag. They showed that in case of staggered tube banks, the heat transfer was augmented by 30–10%, and the corresponding pressure loss was reduced by 55–34% for the Reynolds number ranging from 350 to 2100. Gentry and Jacobi [6] experimentally explored the heat transfer enhancement by delta-wing-generated tip vortices in flat-plate and developing channel flows. They reported that on the complete channel surface the largest spatially averaged heat transfer enhancement was 55% accompanied by a 100% increase in the pressure drop relative to the same channel flow with no delta-wing vortex generator. Leu et al. [7] numerically and experimentally studied the heat transfer and flow in the plate-fin and tube heat exchangers with inclined block shape vortex generators mounted behind the tubes. They pointed out that the proposed heat transfer enhancement technique is able to generate longitudinal vortices and to improve the heat transfer performance in the wake regions. Sommers and Jacobi [8] experimentally investigated the air-side heat transfer enhancement of a refrigerator evaporator using vortex generation. They noted that for air-side Reynolds numbers between 500 and 1300, the air-side thermal resistance was reduced by 35–42% when vortex generation was used. Pesteei et al. [9] experimentally studied the effect of winglet location on heat transfer enhancement and pressure drop in fin-tube heat exchangers. They found that the winglet pairs were most effective to enhance the heat transfer coefficients when these were placed in the downstream side. Hiravennavar et al. [10] numerically studied the flow structure and heat transfer enhancement by a winglet pair of nonzero thickness. They observed that in comparison with a channel without winglets, the heat transfer was enhanced by 33% when single winglet is used and by 67% when a winglet pair was employed. Joardar and Jacobi [11] numerically investigated the flow and heat transfer enhancement using an array of delta-winglet vortex generators in a fin-and-tube heat exchanger. They adopted ''common-flow-up'' arrangement for vortex generators in three different configurations. The 3VG-inline-array configuration achieves enhancements up to 32% in total heat flux and 74% in j factor over the baseline case, with an associated pressure drop increase of about 41%. Wu and Tao [12] investigated the laminar heat transfer in aligned three-row fin-and-tube heat exchangers with longitudinal vortex generators from the viewpoint of field synergy principle.

There are few reports of implementation of longitudinal vortex generators in fin-and-oval-tube heat exchangers in open literature [18].

Chen et al. [13] numerically explored the conjugate heat transfer of a finned-oval tube with a punched longitudinal vortex generator in form of a delta winglet. They mainly focused on one element of the heat exchanger (only one oval tube involved). Based on their work, they further investigated the heat transfer enhancement of finned oval tube with inline longitudinal vortex generators [14] as well as with staggered longitudinal vortex generators [15], and they obtained some useful optimized results. Tiwari et al. [16] numerically studied the laminar flow and heat transfer in a channel with built-in oval tube and delta winglet vortex generators. They revealed that combinations of oval tube and the winglet pairs improved the heat transfer significantly. O'Brien et al. [17] experimentally investigated the forced convection heat transfer in a narrow rectangular duct fitted with an elliptical tube and one or two delta-winglet pairs. They found that the addition of the single winglet pair to the oval-tube geometry yielded significant heat transfer enhancement, averaging 38% higher than the oval-tube, no-winglet case. The corresponding increase in friction factor associated with the addition of the single winglet pair to the oval-tube geometry was moderate.

The foregoing literature review shows that only limited numerical analyses on fin-and-oval-tube heat exchangers with LVGs have been published. The previous investigations were mainly focused on parametric study, and heat transfer enhancement was only explored from the traditional perspective. In fact, that is insufficient to uncover the fundamental causes of heat transfer enhancement. Moreover, most of the previous studies of fin-and-oval-tube heat exchangers with LVGs are focused on single heat transfer element (only one tube involved) [18]. Therefore, P. Chu et al. [18] numerically investigated the heat transfer characteristics and fluid flow structure of fin-and-oval-tube heat exchangers with longitudinal vortex generators (LVGs) for *Re* ranges from 500 to 2500. They found that the average *Nu* for the three-row fin-and-oval-tube heat exchanger with LVGs increased by 13.6–32.9% over the baseline case and the corresponding pressure loss increased by 29.2–40.6%. The study carried out with three geometrical parameters – placement of LVGs (upstream and downstream), angles of attack ($\alpha =$ 15°, 30°, 45° and 60°) and tube-row number (n = 2, 3, 4 and 5). The results show that the LVGs with placement of downstream, angle of attack of 30° and minimum tube-row number provide the best heat transfer performance.

Continually with the last reference, this paper presents a two-dimensional numerical investigation of laminar flow and heat transfer characteristics at constant wall heat flux condition, over a three rows oval-tube bank in staggered arrangement with rectangular vortex generators, for Reynolds number ranging from 250 to 1500. The study focuses on the effects of position and angle of attack of VGs on heat transfer and fluid flow characteristics of oval-tube heat exchanger. Behind each oval-tube, a pair of rectangular winglet VG is situated with placement of downstream. Six different positions (3 in *x*-axis and 2 in *y*-axis) and two angles of attack α (30° and 45°) are investigated. The Influence of the different parameters on heat transfer enhancement (average Nusselt number of tubes), and skin friction coefficient characteristic are studied numerically by the aid of the computational fluid dynamics (CFD) commercial code of FLUENT version 6.3.

2. MODEL DESCRIPTION

2.1. Physical Model

Top view of schematic diagram of a fin-and-oval-tube heat exchanger in staggered arrangement with LVGs is shown in **Fig.(1)**. A pair of rectangular winglets is punched out of the fin surface symmetrically behind each oval tube. Due to the symmetric arrangement, the region occupied by dashed lines is selected as the computational domain, which is, considered as a channel of height $H = 12$ mm and length $L = 75$ mm. The tube rows are arranged in a staggered design.

The span wise tube pitch or the transverse distance between two rows which equivalent the twice of height of the module channel is $P_s = 2H = 24$ mm, and the longitudinal tube pitch or the distance between the tube centers is $P_l = 22$ mm.

The major $2a$ and minor $2b$ diameters of oval tube are 12 mm and 7 mm respectively. The rectangular LVG, of length $w = 4$ mm and thickness $\delta = 0.25$ mm, is located at the six relative distances ($\Delta X/a = 1$, 1.125 and 1.25) and ($\Delta Y/b = 1$ and 1.15) calculated from its front edge to the center of oval tube. In addition, the angles of attack α of LVGs are varied by (30° and 45°).
The actual computation domain is extended by 10H at the inlet to maintain the inlet velocity uniformity and the domain is extended by 30H at the exit to ensure a recirculation-free flow there. The first oval tube is located at $X = 11$ mm from its center to the inlet of channel. The oval tube and rectangular vortex generators parameters are shown in **Fig.(2)** and the studied cases are listed in **Table(1)**.

2.2. Boundary Conditions

All the boundary conditions are given in **Fig.(3)**. The flow was assumed two-dimensional, laminar, steady state and incompressible with constant physical properties. The working fluid is air with constant properties at $Pr = 0.74$. The investigations are performed for Reynolds numbers between 250 and 1500.

- *At the channel inlet*:

    The fluid is assumed to enter with a uniform horizontal velocity U_{in} and temperature T_{in}.
    $U = U_{in}$; $T = T_{in} = 300$ K   ; $V = 0$

- *At the channel outlet*:

    $$P = P_{out} = 101325 \text{ Pa} \quad ; \quad \frac{\partial U}{\partial x} = \frac{\partial V}{\partial x} = \frac{\partial P}{\partial x} = \frac{\partial T}{\partial x} = 0$$

- *Symmetry condition*:

    For the top and bottom surfaces of the computational domain excluding the tube surfaces, symmetry boundary condition is used. The mathematical form of this condition:
    $$\frac{\partial U}{\partial y} = 0 \quad ; \quad V = 0 \; ; \quad \frac{\partial T}{\partial y} = 0$$

- *Oval tube wall surface*:

    $U = V = 0$; $T_w = \text{constant} = 400$ K

- *Rectangular VG wall surface*:

    $U = V = 0$;   wall is no-slip and adiabatic conditions.

2.3. Governing Equations

The governing equations in Cartesian coordinates can be expressed as follows:

Continuity equation:

$$\frac{\partial U}{\partial x} + \frac{\partial V}{\partial y} = 0 \tag{1}$$

Momentum equations:

$$\rho \left(U \frac{\partial U}{\partial x} + V \frac{\partial U}{\partial y} \right) = - \frac{\partial P}{\partial x} + \mu \left(\frac{\partial^2 U}{\partial x^2} + \frac{\partial^2 U}{\partial y^2} \right) \tag{2.1}$$

$$\rho \left(U \frac{\partial V}{\partial x} + V \frac{\partial V}{\partial y} \right) = - \frac{\partial P}{\partial x} + \mu \left(\frac{\partial^2 V}{\partial x^2} + \frac{\partial^2 V}{\partial y^2} \right) \tag{2.2}$$

Energy equation:

$$\rho c_p \left(U \frac{\partial T}{\partial x} + V \frac{\partial T}{\partial y} \right) = k_f \left(\frac{\partial^2 T}{\partial x^2} + \frac{\partial^2 T}{\partial y^2} \right) \tag{3}$$

2.4. Parameter Definitions

The Reynolds number *Re* (based on the hydraulic diameter) is defined as:

$$\text{Re} = \frac{\rho \, U_m \, D_h}{\mu} \tag{4}$$

where U_m is the mean velocity inlet in the minimum flow cross-section of the flow channel, and D_h is the hydraulic diameter which equals to $2H$.

The value of the local Nusselt number Nu_{loc} on the surface of an isothermal oval-tube is evaluated using the temperature field as follows:

$$Nu_{loc} = \frac{h \, 2a}{k} = - \frac{\partial T}{\partial n_s} \tag{5}$$

Where the n_s (the unit vector normal to the surface of the oval-tube) is given as

$$n_s = \frac{(x/a^2) e_x + (y/b^2) e_y}{\sqrt{(x/a^2)^2 + (y/b^2)^2}} = n_x e_x + n_y e_y$$

Where e_x and e_y are the *x*- and *y*-components of the unit vector, respectively.

The average Nusselt number Nu_{av} and skin friction coefficient C_f are defined as:

$$Nu_{av} = \frac{1}{2\pi} \int_0^{2\pi} Nu_{loc}(\theta)\, \partial\theta \tag{6}$$

$$C_f = \frac{\tau_w}{0.5\,\rho U_m^2} \tag{7}$$

Where (θ) is the angular displacement from the front stagnation, and τ_w is the wall shear stress.

3. NUNERICAL METHODS

The commercial computational fluid dynamics code FLUENT was used to solve the governing equations, which were discretized by the finite volume method. The SIMPLE (Semi Implicit Method for Pressure-Linked Equations) algorithm was used for the velocity-pressure coupling. The second-order upwind scheme was employed for the discretization of the convection terms. An unstructured quadrilateral mesh was generated using Gambit 2.0, with fine mesh around the tube and a coarse mesh in the extended regions, as shown in the **Fig.(4)**.

A series of calculations for a single module was performed in order to choose a suitable grid size for the model. For a case with $\Delta X/a = 1.25$, $\Delta Y/b = 1$ and angle of attack $\alpha = 30^o$ at $Re = 500$ (chosen arbitrarily), the grid independency was studied on three different grids size of 3265, 5880 and 12160 cells. The average Nusselt numbers and average skin friction coefficient are listed in **Table(2)**. From the table we can see that the maximum different of the average Nu number and C_f is less than 2% and 1.3% respectively, for three different grid systems. For the present study, the final grid number is selected as about 5900 cells. Similar validations are also conducted for other cases.

4. RESULTS AND DISCUSSION

4.1. Influence of LVGs

In order to study the influence of LVGs on the heat transfer characteristics and the fluid flow over a bank of oval-tubes, a comparative investigation for three oval-tube-rows model with and without LVGs is performed. Firstly, the heat exchanger model without LVGs will be referred to as ''baseline'' case and the heat exchanger with LVGs will be referred to as ''modified'' case as shown in **Fig.(5)**.

For the comparison test, the LVGs are placed in the position of $\Delta X/a = \Delta Y/b = 1$, and the angle of attack is set as 45°. The Re number based on the hydraulic diameter ranges from 250 to 1500. **Fig.(6)** shows the different configurations for oval-tube banks model between the baseline and modified models. It can be seen that the overall Nu_{av} number for both baseline and modified

cases increases with the increasing *Re* number. However, the overall Nu_{av} number for the modified case is improved by 22–27.7% in comparison with the baseline case.

Fig's. (7) illustrates the temperature profiles for baseline case and modified case with two angles of attack, respectively for *Re* = 1000. Comparing the three temperature profiles, we can see that the temperature distribution in the vicinity of the inlet region is almost identical for all cases. As the air approaches the LVGs, the streamwise vortices are generated and the heat transfer from the tubes is significantly enhanced. As we see, the temperature profiles around the tubes surface are different between the baseline case and modified cases due to the streamwise vortices of VGs and the flow acceleration in the region between the VGs and oval-tubes, which it appears more apparent with angle of attack of 45°. Thus, the temperature behind the tube surface for modified cases is distinctly lower than that in the corresponding region for baseline case.

4.2. Effect of LVGs Parameters on Heat Transfer (Nu)

The influence of both positions and angles of attack of LVGs on the heat transfer and fluid flow characteristic for the oval-tube banks is investigated. **Fig.(8)** shows that the overall Nu_{av} number, for both baseline and modified cases, increases with increasing *Re* number at varying the relative distance $\Delta X/a$ and fixing $\Delta Y/b$ and $\alpha = 30^o$. As we see that the increasing of overall Nu_{av} number is decreases with increasing the relative distance $\Delta X/a$ for all *Re* number. The same behavior occurs at the angle $\alpha = 45^o$ with fixing the two relative distances of $\Delta Y/b$ as shown in **Fig.(9)**, but the enhancement in overall Nu_{av} number with the angle of 45° is best comparing with the case in **Fig.(8)**.

From **Fig's. (8 and 9)**, it can be seen that the using of LVGs give the best of enhancement with decreasing the relative distances, where in the Reynolds number range of the present study, the overall Nu_{av} number increases by 10–20.4% with angle of attack 30°, and by 10.4–27.7% with angle of attack 45° comparing with the baseline case. The maximum enhancement of heat transfer from three rows of oval-tube occurs at the positions ($\Delta X/a = 1$ and $\Delta Y/b = 1.15$) and ($\Delta X/a = 1$ and $\Delta Y/b = 1$) with the angles of 30° and 45° respectively.

There are some reasons leading to this high enhancement at these parameters of LVGs. One of these is the influence of vortex generators, which reduce the size of wake region behind each oval tube, and the flow will be accelerating at this narrow region, which be optimum at the lower relative distances. In addition, the vortices generated by VGs around the first tube row will interact with the vortices generated by VGs around the second and third tube rows. It is evident from **Fig.(10)**. that the velocity of air will increases due to the first LVGs, in the regions restricted behind the LVGs and the subsequent oval-tube. This leads to extra enhancement of the heat transfer from the second and third oval-tube rows at high *Re* number. Therefore, the overall Nu_{av} number of the 3-rows of oval- tube will be increase.

Fig's. (11, 12 and 13) show the influence of the LVGs parameters on local *Nu* number (Nu_{loc}) of each oval-tube in the baseline and modified models respectively. From **Fig's. (12 and 13)** it can be observed that the Nu_{loc} increases on the rear surface of each oval-tube due to the VGs in comparison with the baseline case. For all cases, the Nu_{loc} on the first oval-tube surface depends on the position of VGs, while in the second and third oval-tubes, the Nu_{loc} depends on the

location of oval-tube in the bank model in addition of the position of VGs. Where we find the higher and lower enhancement occurs on the second and third oval-tube respectively. The best enhancement on the second oval-tube occurs because of the accelerating of coming airflow due to the VGs behind the first oval-tube, while the decreasing on the third oval-tube occurs because of the rising of coming air temperature.

4.3. Effect of LVGs Parameters on Skin Friction Coefficient (C_f)

The distribution of local skin friction coefficient around each oval-tube is studied. As we know that the flow in the channel with tubes are cause a significant fluid friction in comparison with the smooth channel. **Fig.(14)** shows the local skin friction coefficient C_f on each oval-tube surface of baseline model at $Re = 1000$. We can observe that not very different in local C_f between the tubes.

For the modified model, the VGs increase the skin friction coefficient with increasing Reynolds number when the flow encounters the blockages created by the presence of VGs, and due to the interaction between the tubes and VGs placed which disturb the entire flow field. That is cause more friction than the case without VGs. Therefore, the increasing in Nu_{loc} number accompanied by increasing in pressure drop and the friction factor.

Fig's. (15 and 16) show the effect of variation of positions and angles of VGs on the local C_f distribution for all the modified cases studied. The local C_f increases due to the VGs with decreasing the relative distances of VGs. It is evident from **Fig's. (15 and 16)** that the increasing in the local C_f with attack angle of 45° is higher than the case with attack angle of 30°. In addition, we can see that the large increasing of local C_f occurs on the second and third oval-tube surfaces with attack angle of 45° at small spacing of location of VGs.

On the other hand, **Fig's. (17 and 18)** show the distribution of average skin friction coefficient around each oval-tube in bank versus Re number for all cases. We can find that the average C_f on each oval-tube increases with increasing Re number and decreasing the spacing of VGs for all cases. The maximum increasing in average C_f around the first, second and third oval-tube, at the concomitant enhancement in heat transfer, are (33.3%), (65.6%) and (60.5%) with the angle of 30°, and (36.4%), (85%) and (94.7%) with the angle of 45° respectively in comparison with the baseline case. That is mean the overall average of C_f of three tubes is 53% and 72% with angles of 30° and 45° respectively. As we see, the high influence of the angle 30° is on the second tube row, while with the angle 45° the third tube row is more affected.

This phenomenon may be explained as follows. For the baseline case, the airflow resistance from the inlet to outlet of the heat exchanger comes from the local resistance of the oval-tubes, which plays dominant part of the total pressure drop. When the LVGs are installed, the airflow resistance will come from the tubes and the local resistance of the LVGs. On the one hand, VGs brings about additional form drag, and delays the separation of boundary layer from the oval tube and decrease the wake region behind the tube so that the form drag from the tubes decreases. Therefore, the VGs with attack angle of 45° offers rather larger form drag than that with attack angle of 30° [12]. Thus, the modified model with attack angle of 45° will increase of Nu_{av} number and average C_f of each oval-tube row.

5. CONCLUSIONS

The fluid flow and heat transfer over a three rows oval-tube bank in staggered arrangement with variation of parameters of LVGs, for Reynolds number (from 250 to 1500), were studied numerically. The main results include:

1. The LVGs enhance the heat transfer on the oval-tubes bank. Scanty difference in enhancement of heat transfer obtained by varying the locations and angles of attack of VGs, where the study shows that the enhancement of overall Nu_{av} number decreases with increasing the relative distances of VGs. On the other hand, the average C_f increases with increasing Re number and decreasing the spacing of locations of VGs.

2. For three-rows of oval-tube bank with VGs, the overall Nu_{av} number is augmented by 10–20.4% with angle of attack 30°, and by 10.4–27.7% with angle of attack 45°, and the average skin friction coefficient C_f on the first, second and third oval-tube increases by (33.3%), (65.6%) and (60.5%), and by (36.4%), (85%) and (94.7%) with the angles of 30° and 45° respectively, in comparison with the baseline case.

3. The average C_f takes a maximum values on the second oval-tube with angle of attack 30°, and on the third oval-tube with angle of attack 45° at small distances of location of VGs.

4. The best locations of the VGs observed at ($\Delta X/a = 1$, $\Delta Y/b = 1.15$) and at ($\Delta X/a = \Delta Y/b = 1$) with the attack angles of 30° and 45° respectively. Where the best average enhancement in heat transfer from the three oval-tubes is about 20.4% and 28%, with an increasing in overall average C_f reached to 53% and 72% for two angles of 30° and 45° respectively, in comparison with the baseline case.

5. The high different in increasing in C_f between the two angles leads to nomination the angle of 30° with small spacing of locations of VGs as an optimum parameters for the model studied.

6. REFERENCES

[1]. F.J. Edwards, G.J.R. Alker, "The improvement of forces convection surface heat transfer using surfaces protrusions in the form of (A) cubes and (B) vortex generators", in: Proceedings of the 5th International Conference on Heat Transfer, Tokyo, vol. 2, pp. 244–248, 1974.

[2]. C.M.B. Russell, T.V. Jones, G.H. Lee, "Heat transfer enhancement using vortex generators, in: , Proceedings of the Seventh Heat Transfer Conference, 3. Hemisphere, New York, pp. 283–288, 1982.

[3]. G. Biswas, N.K. Mitra, M. Fiebig, "Heat transfer enhancement in fin tube heat exchangers by winglet type vortex generators". Int. J. Heat Mass Transfer 37, pp. 283-291, 1994.

[4]. A.A.B. Jahromi, N.K. Mitra, G. Biswas, "Numerical investigations on enhancement of heat transfer in a compact fin-and- tube heat exchanger using delta winglet type vortex generators". J. Enhanced Heat Transfer 6, pp. 1–11, 1999.

[5]. K. Torii, K.M. Kwak, K. Nishino, "Heat transfer enhancement accompanying pressure-loss reduction with winglet-type vortex generators for fin-tube heat exchangers", Int. J. Heat

Mass Transfer 45, pp. 3795–3801, 2002.

[6]. M.C. Gentry, A.M. Jacobi, "Heat transfer enhancement by delta-wing- generated tip vortices in flat-plate and developing channel flows", J. Heat Transfer 124, pp. 1158–1168, 2002.

[7]. Jin-Sheng J.-S. Leu, Ying-Hao Y.-H. Wu, Jiin-Yuh J.-Y. Jang, "Heat transfer and fluid flow analysis in plate-fin and tube heat exchangers with a pair of block shape vortex generators", Int. J. Heat Mass Transfer 47, pp. 4327–4338, 2004.

[8]. A.D. Sommers, A.M. Jacobi, "Air-side heat transfer enhancement of a refrigerator evaporator using vortex generation", Int. J. Refrig. 28, pp. 1006–1017, 2005.

[9]. S.M. Pesteei, P.M.V. Subbarao, R.S. Agarwal, "Experimental study of the effect of winglet location on heat transfer enhancement and pressure drop in fin-tube heat exchangers", Appl. Therm. Eng. 25, pp. 1684–1696, 2005.

[10]. S.R. Hiravennavar, E.G. Tulapurkara, G. Biswas, "A note on the flow and heat transfer enhancement in a channel with built-in winglet pair", Int. J. Heat Fluid Flow 28, pp. 299–305, 2007.

[11]. A. Joardar, A.M. Jacobi, "A numerical study of flow and heat transfer enhancement using an array of delta-winglet vortex generators in a fin-andtube heat exchanger", J. Heat Transfer 129, pp. 1156–1167, 2007.

[12]. J.M. Wu, W.Q. Tao, "Investigation on laminar convection heat transfer in finand- tube heat exchanger in aligned arrangement with longitudinal vortex generator from the viewpoint of field synergy principle". Appl. Therm. Eng. 27, pp. 2609–2617, 2007.

[13]. Y. Chen, M. Fiebig, N.K. Mitra, "Conjugate heat transfer of a finned oval tube with a punched longitudinal vortex generator in form of a delta winglet–parametric investigations of the winglet", Int. J. Heat Mass Transfer 41, pp. 3961–3978, 1998.

[14]. Y. Chen, M. Fiebig, N.K. Mitra, "Heat transfer enhancement of a finned oval tube with punched longitudinal vortex generators in-line", Int. J. Heat Mass Transfer 41, pp. 4151–4166, 1998.

[15]. Y. Chen, M. Fiebig, N.K. Mitra,"Heat transfer enhancement of finned oval tube with staggered punched longitudinal vortex generators", Int. J. Heat Mass Transfer 43, pp. 417–435, 2000.

[16]. S. Tiwari, D. Maurya, G. Biswas, V. Eswaran, "Heat transfer enhancement in cross-flow heat exchangers using oval tubes and multiple delta winglets", Int. J. Heat Mass Transfer 46, pp. 2841–2856, 2003.

[17]. James E.J.E. O'Brien, Manohar S.M.S. Sohal, Philip C.P.C. Wallstedt, "Local heat transfer and pressure drop for finned-tube heat exchangers using oval tubes and vortex generators", J. Heat Transfer 126, pp. 826–835, 2004.

[18]. P. Chu, Y.L. He, Y.G. Lei, L.T. Tian, R. Li, "Three-dimensional numerical study on fin-and-oval-tube heat exchanger with longitudinal vortex generators", Applied Thermal Engineering 29, pp. 859–876, 2009.

NOMENCLATURE

a	semi- major diameter of oval tube (m)	*Greek symbols*	
b	semi-minor diameter of oval tube (m)	α	angle of attack (°)
C_f	skin friction coefficient	δ	thickness of LVG
c_p	specific heat (J/kg K)	θ	angular displacement (°)
D_h	hydraulic diameter, $D_h = 2H$	μ	viscosity (kg/(m s))
H	channel height (m)	v	kinematic viscosity (m²/s)
k	thermal conductivity (W/m K)	ρ	density (kg/m³)
L	computational domain length (m)	τ	shear stress (Pa)
Nu	Nusselt number, $= h\,D_h\,/\,k$	ΔX	streamwise distance (m)
P	pressure (Pa)	ΔY	spanwise distance (m)
P_l	longitudinal tube pitch (m)		
P_s	span wise tube pitch (m)	*Subscripts*	
Pr	Prandtl number, $= \mu\,c_p\,/\,k$	av	average
Re	Reynolds number, $= U_m D_h /v$	in	inlet parameter
T	temperature (K)	loc	local
T_{in}	inlet temperature (K)	out	outlet parameter
T_w	wall temperature (K)	w	wall
U_m	mean velocity inlet (m/s)		
U,V	velocity components (m/s)	*Abbreviations*	
w	length of LVG	LVGs	longitudinal vortex generators
x,y	Cartesian coordinates	VG	vortex generator

Table (1): Geometric parameters of the VGs for the studied cases.

Case No.	α ($^{\circ}$)	$\Delta X/a$	$\Delta Y/b$
1	30	1	1
2	30	1.125	1
3	30	1.25	1
4	30	1	1.15
5	30	1.125	1.15
6	30	1.25	1.15
7	45	1	1
8	45	1.125	1
9	45	1.25	1
10	45	1	1.15
11	45	1.125	1.15
12	45	1.25	1.15

Table (2): Grid independent test.

	Grid Size/cell		Diff.	Grid Size/cell	Diff.
	3265	**5880**	**%**	**12160**	**%**
Nu_{av}	12.871	12.788	0.65	12.579	1.66
C_f	0.0190749	0.01888343	1.01	0.01864908	1.26
% Diff. = [(Grid I)–(Grid II)] · 100/(Grid II)					
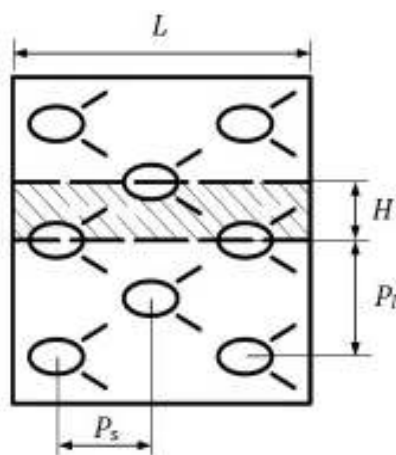
Fig. 1. Schematic diagram of computational domain
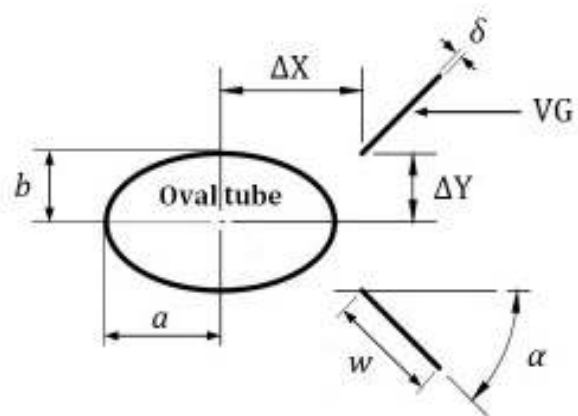
Fig. 2. Oval tube and VGs parameters
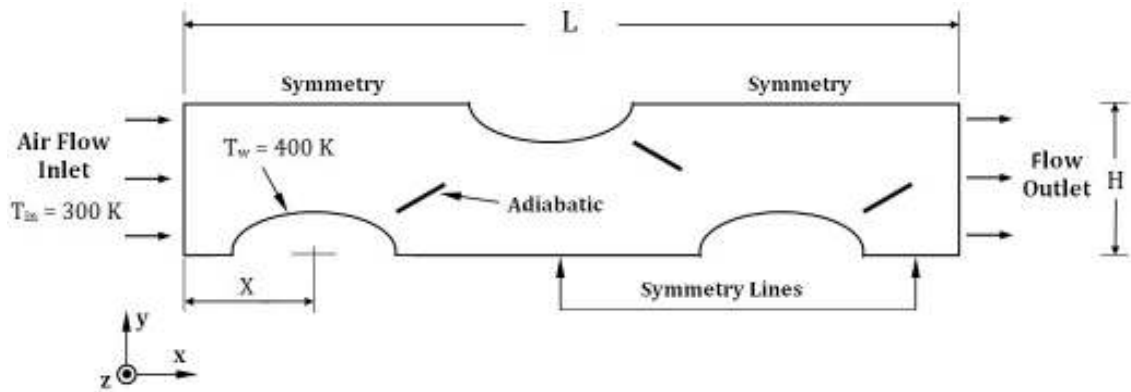
Figure(3): The computational domain and boundary conditions.
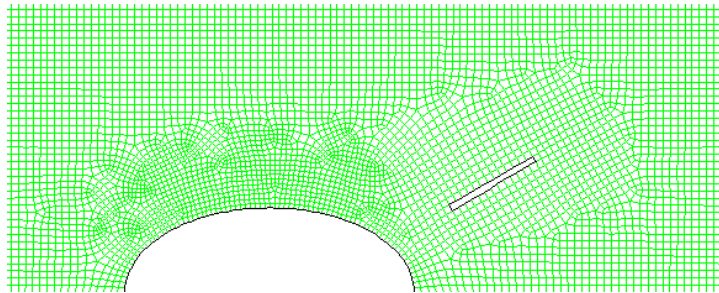
Figure(4): Grid system around the oval-tube with VG.
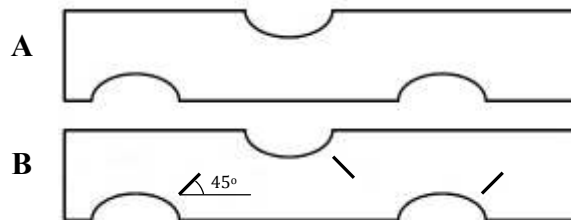
Figure(5): Different configurations for 3-rows oval-tube bank with and without LVGs: (**A**) baseline case, (**B**) modified case.
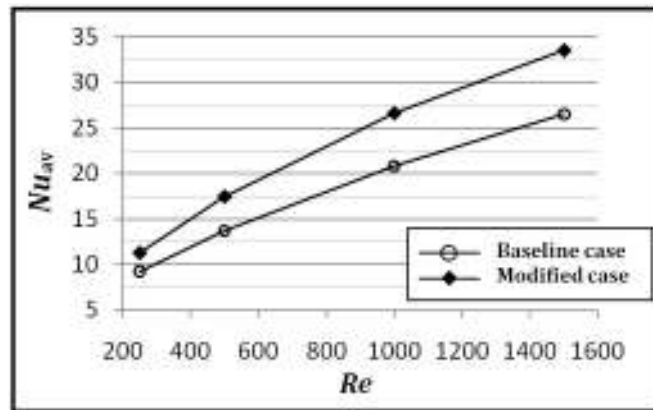
Figure(6): Influence of LVGs on the average *Nu* number for two cases.
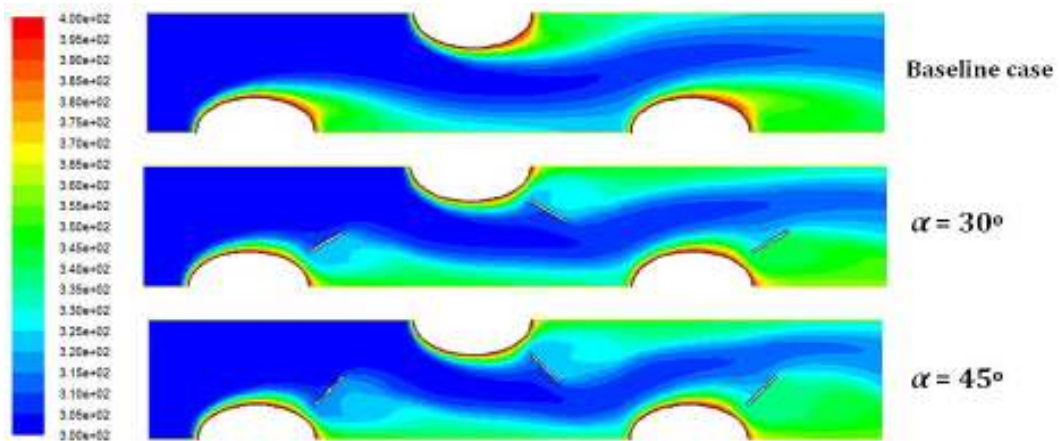
Figure(7): Temperature distribution on the three rows oval-tube bank for both baseline and modified cases at the position $\Delta X/a = \Delta Y/b = 1$, and two angles of attack, for *Re* = 1000.
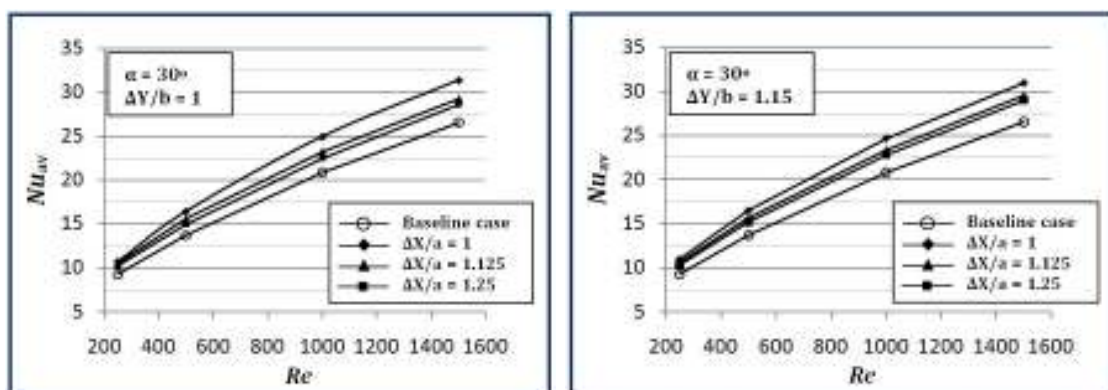
Figure(8): Influence of relative distance ($\Delta X/a$) on the overall Nu_{av} at angle of attack $\alpha = 30^o$ and fixing ($\Delta Y/b$) at 1 and 1.15.
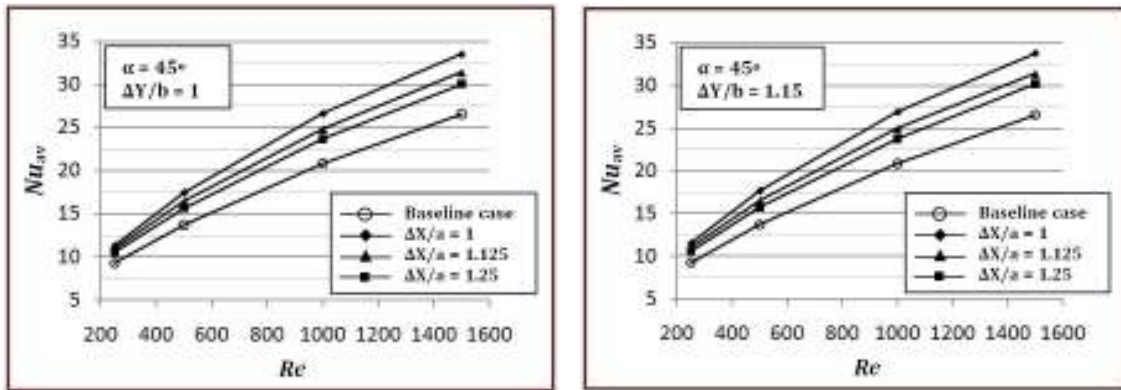
Figure(9): Influence of relative distance (ΔX/*a*) on the overall *Nu*av number at angle of attack α =
45°
and fixing (ΔY/*b*) at 1 and 1.15.
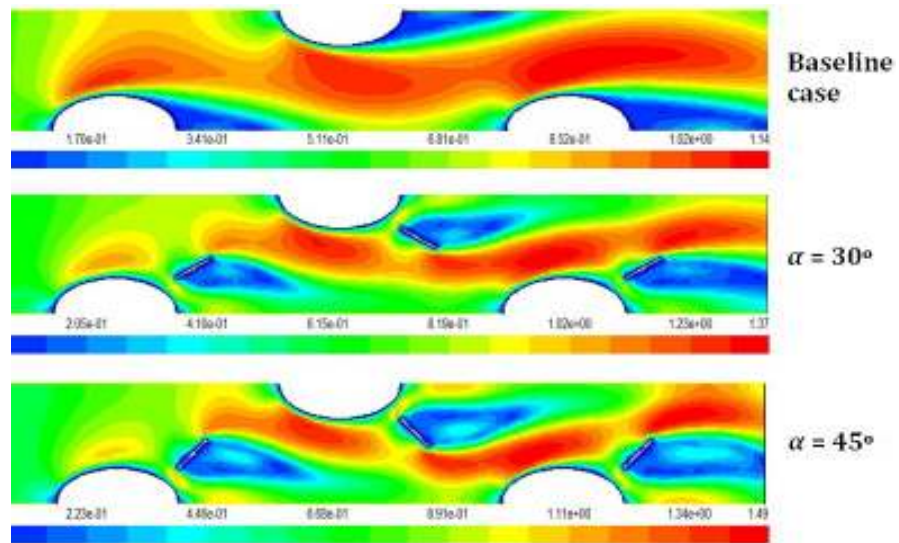
Figure(10): Velocity distribution on the three rows oval-tube bank for baseline and modified
models at the position ΔX/*a* = ΔY/*b* = 1, and two angles of attack, for *Re* = 1000.

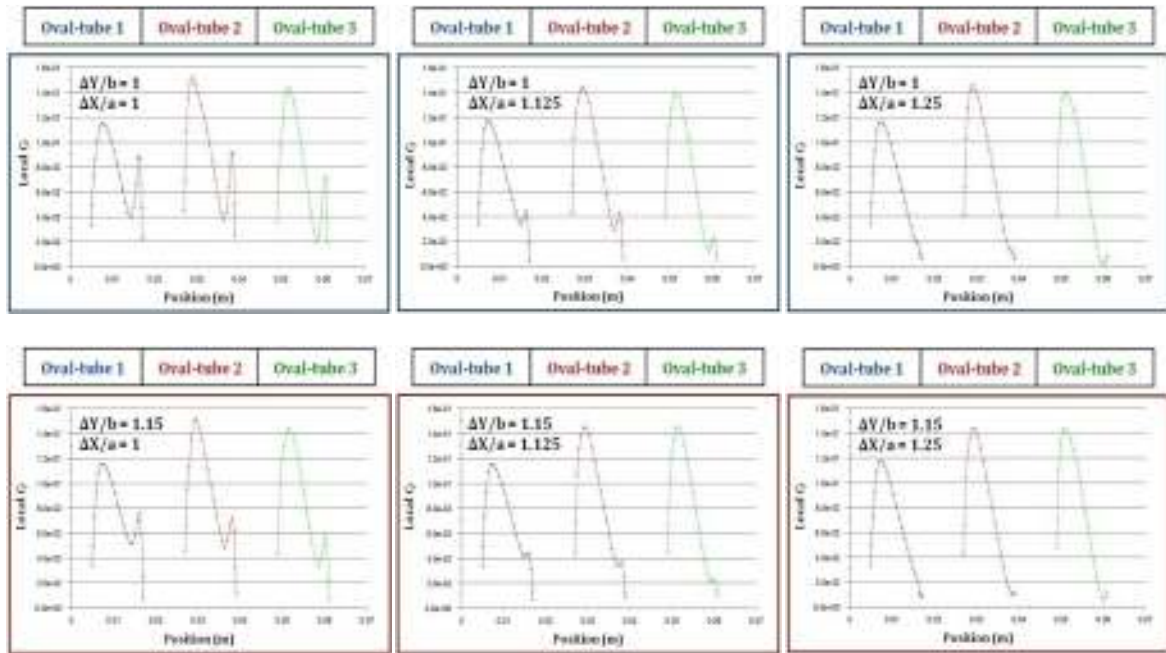**Figure(11):** Local *Nu* number on each oval-tube surface for the baseline model at *Re* = 1000.
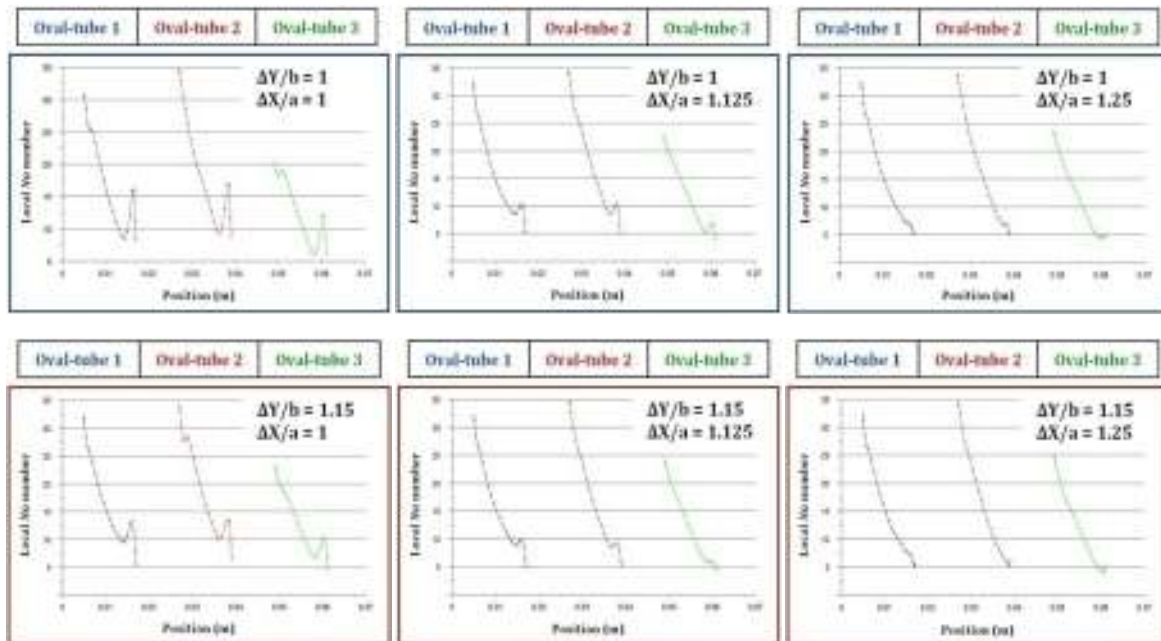
Figure(12): Effect the variation of positions of VGs on local *Nu* number of each oval-tube surface for the modified model with angle of attack *α* = 30° and *Re* = 1000.
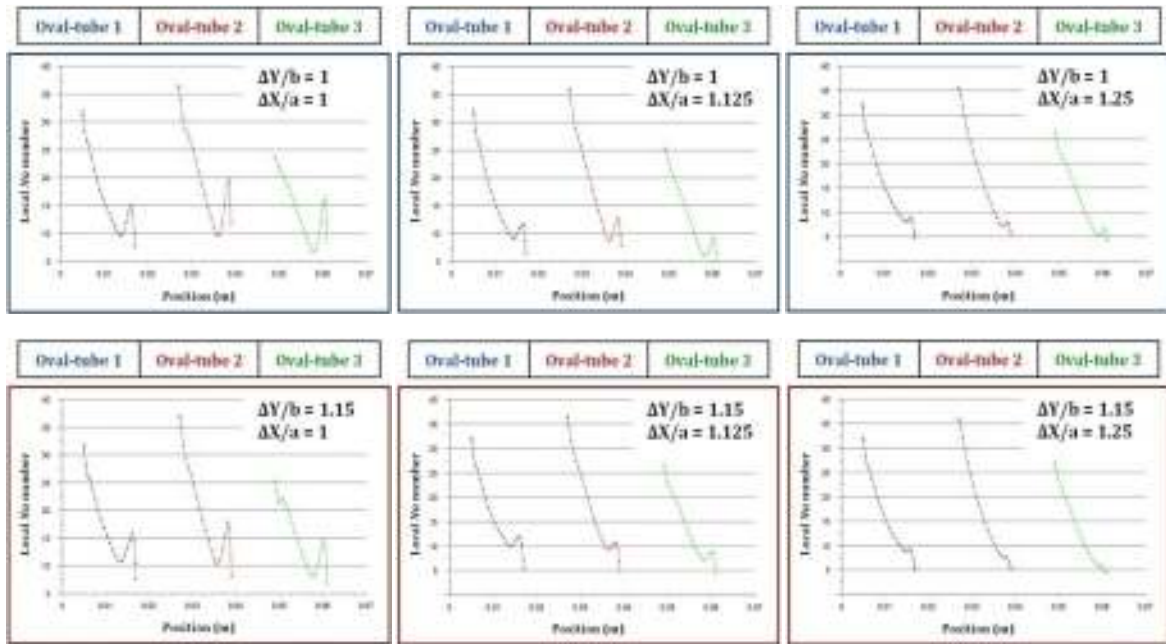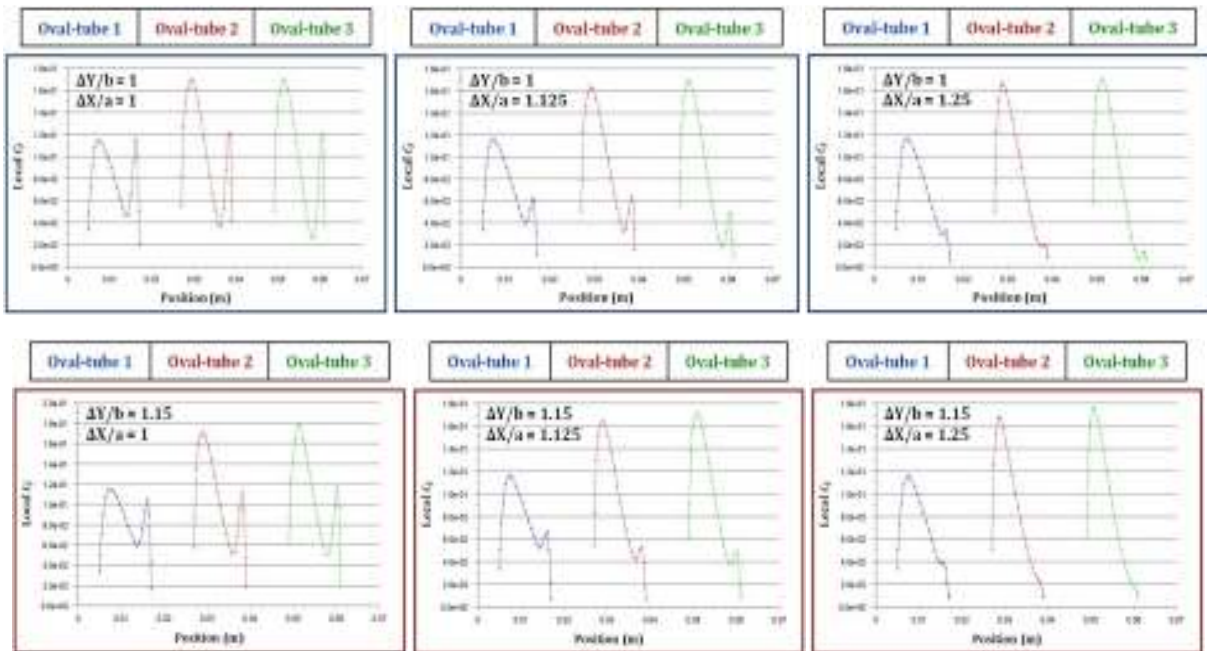
Figure(13): Effect the variation of positions of VGs on local *Nu* number of each oval-tube surface for the modified model with angle of attack $\alpha = 45^\circ$ and *Re* = 1000.
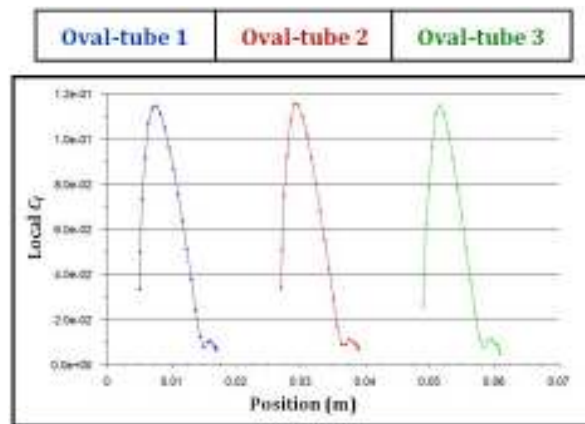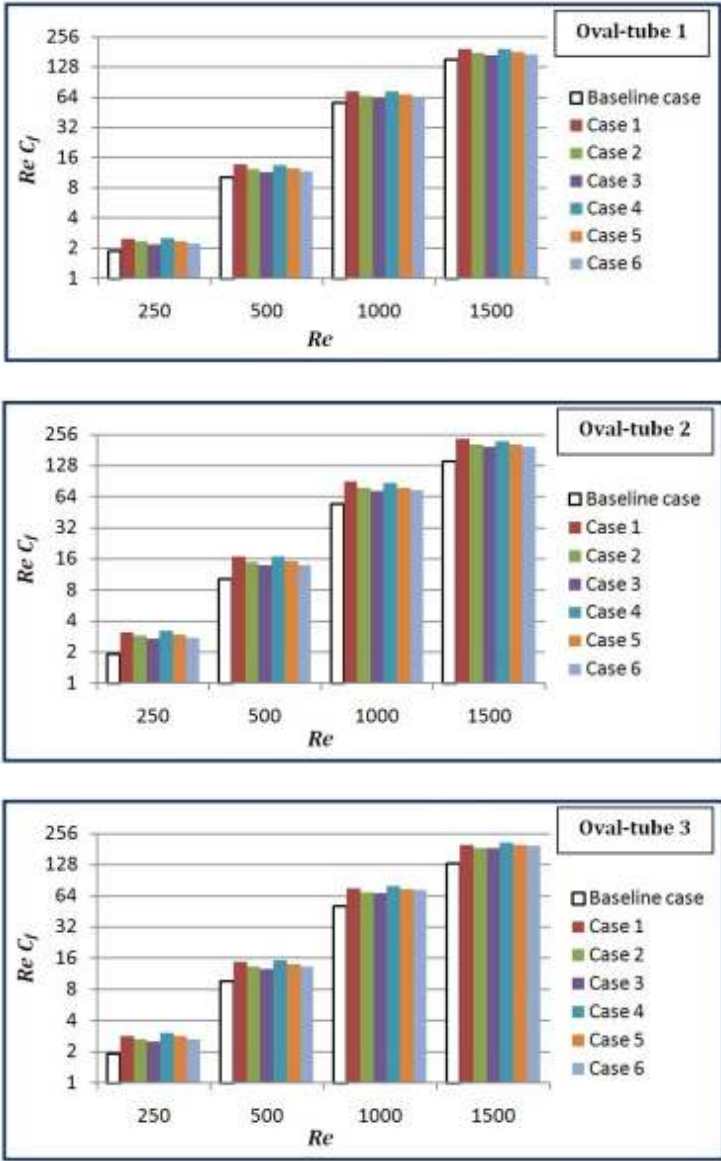

Figure(14): Local skin friction coefficient around each oval-tube of baseline model at *Re* = 1000.

Figure(15): Effect the variation of positions of VGs on local skin friction coefficient (C_f) of each oval-tube surface for the modified model with angle of attack $\alpha = 30^o$ and $Re = 1000$.

Figure(16): Effect the variation of positions of VGs on local skin friction coefficient (C_f) of each oval-tube surface for the modified model with angle of attack $\alpha = 45^o$ and $Re = 1000$.

Figure(17): The distribution of average skin friction coefficient (C_f) around each oval-tube with attack angle of 30°.
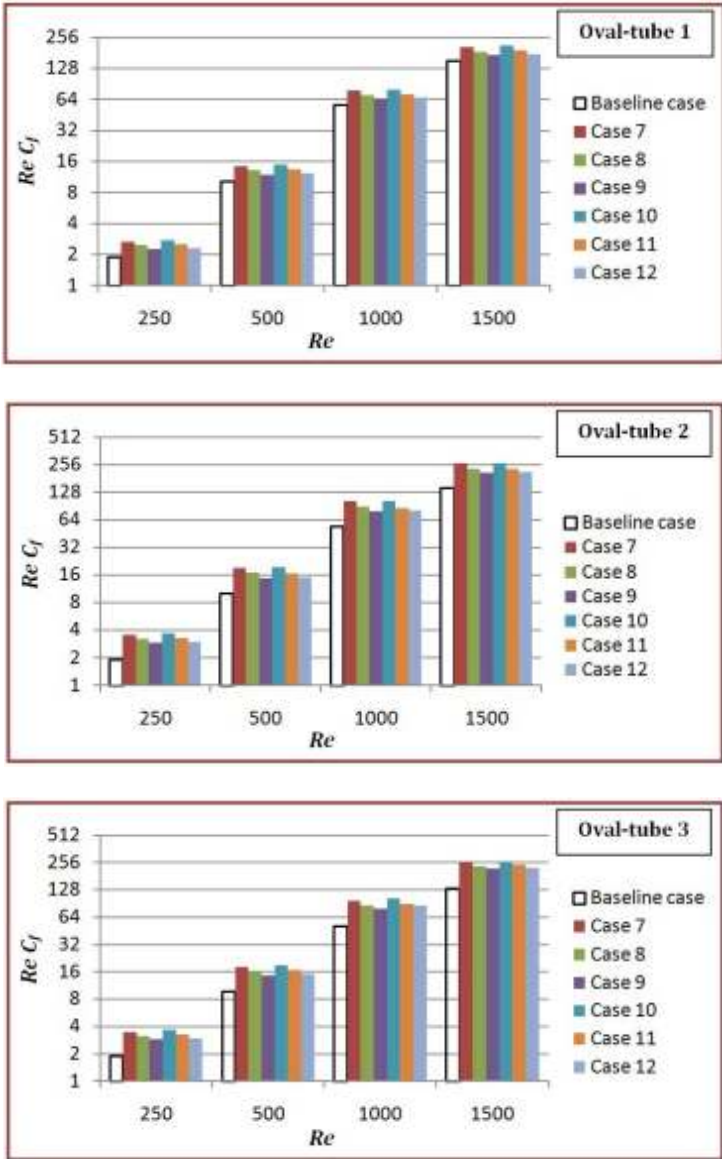
Figure(18): The distribution of average skin friction coefficient (C_f) around each oval-tube with attack angle of 45º.

دراسة عددية للجريان وانتقال الحرارة في مبادل حراري من صف من الأنابيب البيضوية بوجود مولدات الدوامة

م.م.عبد المجيد عبد الحميد رمضان

قسم الهندسة الميكانيكية

كلية الهندسة– جامعة الأنبار

الخلاصـة

يتناول البحث المقدم دراسة عددية ثنائية البعد لجريان طباقي لفحص خواص الجريان وانتقال الحرارة لثلاثة صفوف من أنابيب بيضوية الشكل (عند ثبوت درجة حرارة السطح) مرتبة بشكل متخالف بوجود زوج من مولدات الدوامة مستطيلة المقطع إلى الخلف من كل أنبوب. ركزت الدراسة التي أجريت ضمن مدى عدد رينولدز (250-1500) على تأثير مواقع وزوايا الهجوم لمولدات الدوامة على تحسين انتقال الحرارة وتأثيرها في معامل الاحتكاك السطحي للأنابيب. تم اختيار ستة مواقع (ثلاثة باتجاه الجريان واثنان باتجاه متقاطع معه) تمثلت في ست مسافات نسبة إلى نصفي قطري الشكل البيضوي، إضافة إلى اختيار زاويتي هجوم (30°) و (45°). تم حل المعادلات الحاكمة باستخدام البرنامج العددي المسمى (FLUENT 6.3) مع اعتبار الجريان انسيابي والحالة مستقرة. أظهرت الدراسة تحسناً في انتقال الحرارة ممثلاً بمعدل عدد نسلت للأنابيب بسبب وجود مولدات الدوامة مقارنة مع الحالة في عدم وجودها، وأن هذا التحسن يقل بزيادة المسافات النسبية لمواقع مولدات الدوامة. حيث بلغ أعلى تحسن نسبي في المعدل الإجمالي لعدد نسلت (20.4%) و (27.7%) عند المسافات النسبية الصغيرة مع زاويتي لهجوم (30°) و (45°) على التوالي. وأن الزيادة في المعدل الإجمالي لمعامل الاحتكاك السطحي للأنابيب الثلاثة المرافقة للتحسن في انتقال الحرارة بلغت (53%) و (72%) لزاويتي الهجوم أعلاه على التوالي.